Front. Earth Sci. 2019, 13(4): 808–816
https://doi.org/10.1007/s11707-019-0792-6

RESEARCH ARTICLE

Large-scale characteristics of landfalling tropical cyclones with abrupt intensity change

Qianqian JI[1,2], Feng XU (✉)[1,2,3], Jianjun XU (✉)[1,2,3], Mei LIANG[1,2], Shifei, TU[1,2], Siqi, CHEN[1,2]

1 South China Sea Institute of Marine Meteorology, Guangdong Ocean University, Zhanjiang 524088, China
2 College of Ocean and Meteorology, Guangdong Ocean University, Zhanjiang 524088, China
3 Southern Marine Science and Engineering Guangdong Laboratory, Zhanjiang 524088, China

© Higher Education Press and Springer-Verlag GmbH Germany, part of Springer Nature 2019

Abstract Data from the China Meteorological Administration and ERA-Interim are used to examine the environmental characteristics of landfalling tropical cyclones (TCs) with abrupt intensity change. The results show that, of all 657 landfalling TCs during 1979–2017, 71%, 70% and 65% of all landfalling TDs, TSs and TYs, respectively, intensify. Of all the 16595 samples, 4.0% and 0.2% of typhoons and tropical storms, respectively, experience over-water rapid intensification (RI) process during their life cycle. Meanwhile, 4.5% and 0.6% of typhoons and tropial storms, respectively, undergo over-water rapid decay (RD). These two kinds of cases, i.e., RI and RD, are used to analyze their associated large-scale conditions. Comparisons show that the RI cases are generally on the south side of the strong western Pacific subtropical high (WPSH); warm sea surface temperatures (SSTs) and sufficient water vapor fluxes existing in RI samples is a dominant feature that is conducive to the development of TCs. Also, the moderate low-level relative vorticity is favorable for TC intensification. On the contrary, the RD TCs are located on the west side of the WPSH; significant decreasing SSTs and low-level water vapor transport may synergistically contribute to RD. Simultaneously, low-level relative vorticity seems to be unfavorable for the development of TCs.

Keywords landfalling tropical cyclone, abrupt intensity change, environmental factors, dynamic composite analysis

1 Introduction

Tropical cyclones (TCs) are one of the most devastating and common disaster types on Earth, and have catastrophic impacts on people's lives and property in coastal areas (Zhang et al., 2009). Accurate forecasts of TC activity can effectively avoid unnecessary social and economic losses. The forecasting accuracy of TC tracks has improved significantly over the past several years (Elsberry, 2014). However, fairly large errors remain in the prediction of TC intensity, especially with respect to abrupt intensity change (Elsberry et al., 2007). Indeed, such a phenomenon remains one of the most challenging tasks faced by forecasters. Therefore, it is important to gain a clear understanding of the characteristics related to TCs with abrupt intensity change. Such research will provide effective guidance for improving TC intensity forecasts.

The role played by ocean heat in the development and maintenance of TC intensification has been identified (e.g., Emanuel et al., 2004). Lowag et al. (2008) concluded that Hurricane Bret's rapid intensification (RI) process was related high sea surface temperatures (SSTs). Warm SSTs of about 27°C and large upper-ocean heat content are two necessary factors for RI (Chan et al., 2001; Lin et al., 2005). Particularly, most intense TCs have been found to undergo RI over regions with high TC heat potential associated with warm eddies (Chan et al., 2001; Lin et al., 2005; Pun et al., 2011).

There have also been many studies revealing the importance to RI of inner-core processes. As described by Willoughby et al. (1982), a TC's outer and inner eyewall replacement process may cause a significant increase in TC intensity. Jiang (2012) suggested that TC intensity changes are indeed related to inner-core convective activity, and it is convective intensity that can influence the rate of intensification. Another factor

Received March 27, 2019; accepted September 9, 2019

E-mails: xuf@gdou.edu.cn, jxu@gdou.edu.cn

affecting TC intensity changes that cannot be ignored is its interaction with the forcing of the large-scale environment. Vertical wind shear can seriously affect TC intensity, and low vertical wind shear is conducive to storm development (Gray, 1967; Merrill, 1988). In addition, upper-level forcing from troughs has an influence on regulating TC intensity change (Pfeffer and Challa, 1981). However, modeling and observational results show that RI can also occur when there is no environmental forcing from upper-level troughs (Emanuel, 1999). These results indicate that external forcing from upper-level systems is likely a factor, but not necessary, for RI. Notably, the three main factors outlined above that are involved in TC intensity changes — ocean heat content, inner-core processes and environmental forcing — have mostly been discussed separately in the literature, with researchers generally choosing to focus only on one of these key aspects. An exception was Bosart et al. (2000), who examined the RI process of Opal (1995) and concluded that it was the combination of environmental forcing and ocean heat content that led to Opal's RI.

Aside from the above studies, other researchers have paid attention to RI more explicitly. For instance, Kaplan and DeMaria (2003) used 12 years of Atlantic TC samples, statistically defining RI by a maximum wind speed increase of at least 30 kt within 24 h, to indicate the environmental conditions that are conducive to RI occurrence; that is, low vertical wind shear, weak forcing from upper-level troughs, warm SSTs, and high relative humidity in the middle-to-low troposphere. Considering the RI occurrence in the western North Pacific (WNP), it has been found that external effects from the environment are more important than internal processes. Yuan and Jiang (2010) used the same method as Kaplan and DeMaria (2003) to develop an RI index for appraising the possibility of RI happening over the next 24 h. However, there was a flaw insofar as the degree to which conditions are favorable for RI was neglected. A revised RI index was subsequently defined based on that original study (Kaplan et al., 2010), and their results showed that the large-scale environmental impact factors are different in the Atlantic and eastern North Pacific basins. Shu et al. (2012) examined the RI process of WNP TCs and found that RI cases were farther from their maximum potential intensity compared with non-RI cases.

Most of the previous research mentioned above did not focus explicitly on the abrupt intensity change process of landfalling TCs. There is no doubt that the majority of damage caused by TCs is associated with TC landfall, and an abrupt change in TC intensity can seriously affect the accuracy of tropical weather forecasting. If a system is undergoing RI or rapid decay (RD) when making landfall and an accurate prediction is unavailable, huge damage to property and heavy losses of life might occur. Therefore, a better understanding of RI and RD is necessary for exploring the mechanisms responsible for TC variability.

The first goal of this paper is to statistically analyze the intensity-change characteristics of landfalling TCs in the WNP over the past 39 years. Then, we seek to distinguish the environmental conditions associated with RI from those cases favorable for RD, in order to provide a basis for the forecasting of such TCs. The data and methods employed are described in Section 2. Section 3 discusses a statistical analysis of the landfalling TCs' 24-h intensity change (ΔV_{24}). A comparison of the conditions present during RI to those during RD is presented in Section 4. Finally, some key conclusions are offered in Section 5.

2 Data and analysis

The best-track data set used in this paper is from the China Meteorological Administration (CMA), including all TCs that occurred in the WNP from 1979 to 2017. The data set comprises records taken four times a day (at 00:00, 06:00, 12:00 and 18:00 UTC), including the central pressure, 6-h estimates of position, and maximum sustained surface wind speed (VMX). Other best-track data sets, acquired from the Joint Typhoon Warning Center and the Regional Specialized Meteorological Center of the Japan Meteorological Agency, are used to validate our results. In this study, a TC is defined as making landfall when its center crosses the coastline at least once during its lifetime. According to the CMA's latest national standard for classifying TCs, the 657 landfalling TCs from 1979 to 2017 are divided into three grades, i.e., tropical depressions (TDs; $10.8 \leqslant \text{VMX} \leqslant 17.1$ m/s), tropical storms (TSs; $17.2 \leqslant \text{VMX} \leqslant 32.6$ m/s) and typhoons (TYs; $\text{VMX} \geqslant 32.7$ m/s), and their numbers are 73, 247 and 337, respectively.

To better coincide with the 95th percentile of ΔV_{24} in the WNP, a critical value of intensity change of 15 m/s within 24 h is employed to identify RI events, as suggested by Shu et al. (2012). Similarly, a 15 m/s threshold is chosen to define RD events in this study, following Wood and Ritchie (2015). Huang and Liang (2010) indicated that the effect of topography on TC intensity usually occurs 6–9 h prior to landfall. To avoid the effects of topography on intensity changes, the sample is further limited by only considering 24-h periods in which the TC center remains more than 200 km from the nearest landmass, as suggested by Liang et al. (2018). This produces a sample size of 420 RI and 522 RD cases in the WNP.

Atmospheric variables are obtained from the ERA-Interim data set, at 6-h intervals and a horizontal resolution of $0.75° \times 0.75°$ (Simmons, 2006). Optimum interpolation SST data at a daily, 0.25° resolution (Reynolds et al., 2007) are obtained from NOAA. Each variable is evaluated using the dynamic composite method, at the beginning and end of each 24-h period, providing that the system undergoes abrupt intensity change during the over-water 24 h before making landfall. The composite range is an area of $30° \times$

30°, centered on the TCs, with the TC center as the coordinate origin, and the x-axis and y-axis are the zonal and meridional directions, respectively.

3 Intensity change distribution

Figure 1 shows the frequency distribution of ΔV_{24} for each TC grade. Slow intensification ($0 \leqslant \Delta V_{24} < 5$ m/s) occurs most frequently for all ΔV_{24} classes, indicating TCs intensify during most of their lifetime. It is found that there is a relatively higher proportion of TSs than TYs and TDs when the ΔV_{24} ranges from 5 to 10 m/s. One plausible reason is that TSs tend to have a larger potential to rapidly intensify than TYs because of a weaker intensity that is further from their maximum possible intensity. The figure also indicates that there is a higher proportion of TYs than any other grade when the ΔV_{24} exceeds 10 m/s. In addition, TYs decay at a fastest rate for all intensity classes ($\Delta V_{24} \leqslant 5$ m/s). Such results may be partially due to the stronger initial intensities (the intensity of a system when it first reaches the TC grade) of TYs than either TSs or TDs, and hence an increased potential for TYs to change rapidly. Table 1 summarizes the ΔV_{24} distributions of all samples. There are 657 landfalling TCs providing a total number of 16595 cases based on a 6-h estimation interval, among which the TY sample contributing 11103 cases is the largest fraction. Also, the TY sample has the widest range of intensity and standard deviation among the three grades. In terms of the mean intensity change in ΔV_{24}, it is positive for both TYs and TSs, but negative for TDs, suggesting that TCs with higher initial intensities have more potential to intensify.

The over-water RI and RD cases in this study consist of 196 TCs, as compared to the total number of 657 landfalling TCs. Abrupt intensity change does not occur in the TD (73) class, probably due to its weak initial intensity. Since RI or RD may occur more than once during a TC's lifecycle, these 196 TCs contribute a total of 420 RI and 522 RD over-water cases. We statistically analyze all over-water RI and RD cases in each intensity-change class and the distribution of ΔV_{24}, and the results indicate that TYs account for a larger proportion than TSs in either RI or RD cases. Most TYs intensify with a ΔV_{24} in the range of

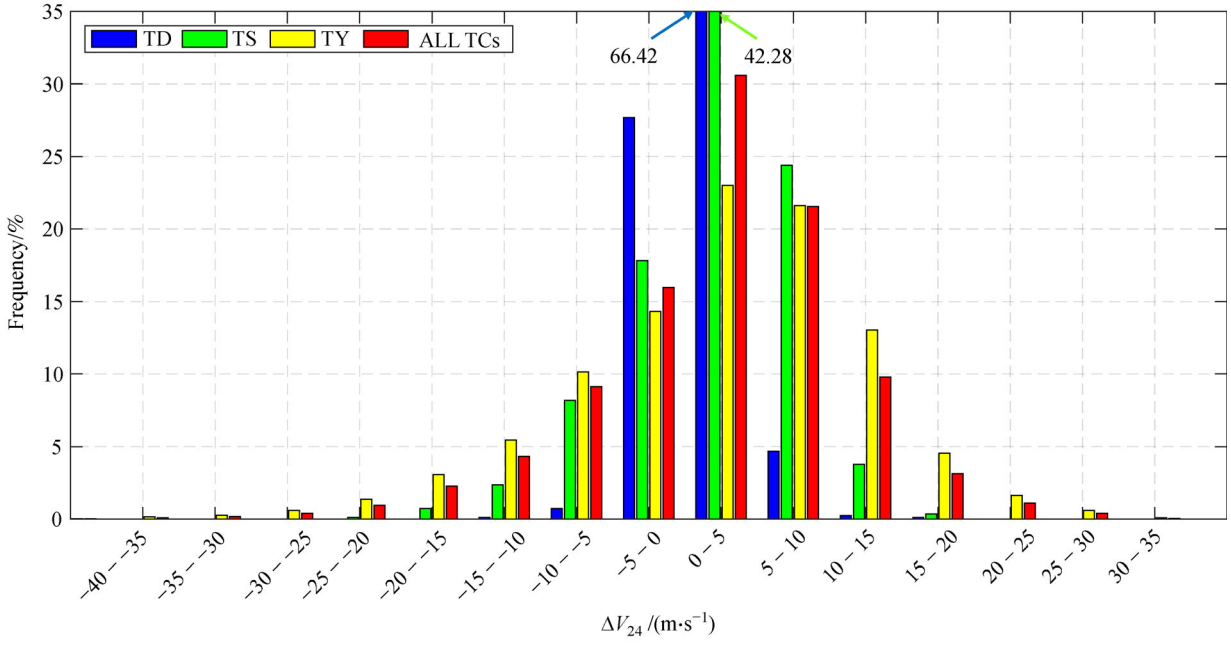

Fig. 1 Frequency distribution of the ΔV_{24} in each TC grade.

Table 1 The ΔV_{24} statistics of TDs, TSs, TYs, and all TC intensity classes. The number of cases (N), mean, standard deviation (std dev), minimum (min), and maximum (max) ΔV_{24} are also provided

Intensity class	N	Mean/(m·s^{-1})	Std dev/(m·s^{-1})	Min/(m·s^{-1})	Max/(m·s^{-1})
TD	831	−0.12	2.5	−12	15
TS	4661	0.37	5.49	−25	16
TY	11103	0.48	9.87	−47	45
All TCs	16595	0.41	8.6	−47	45

15–20 m/s, and weaken with a ΔV_{24} from –20 to –15m/s. The number of RI and RD cases is normalized by class sample size to remove the variations in each intensity grade, and the possibility of a system to undergo over-water abrupt intensity change is still the largest for the TYs. Specifically, about 4.0% and 0.2% of the TY and TS samples, respectively, go through RI; similarly, 4.5% and 0.6% of TY and TS samples experience RD.

From the distribution of over-water 24-h tracks of RI and RD processes in which the TC center remains more than 200 km from the nearest landmass (not shown), we can see the RI events most often occur in the region of 10°N–20°N, and these cases mainly move to the north-west. East of the Philippines (10°N–15°N, 130°E) is the region with the most frequent occurrence of RI cases, while RI cases rarely occur in the South China Sea. In terms of seasonal distribution, the majority of RI cases (nearly 28%) occur in July and August (25%), with a slightly larger fraction than in September (24%) or October (11%). More RD cases occur in areas close to the coast compared with open-ocean, and they move to the north-west mostly. RD cases occur mostly in September (about 29%), followed by August (25%), July (22%), and then October (13%).

4 Large-scale conditions associated with RI and RD cases

According to the rapid intensity change criteria mentioned above, the samples are further limited by only considering 24-h periods during which the TC center remains at least 200 km from the nearest landmass. Two types of TCs are selected to compare the environmental conditions through dynamic composite analysis at the beginning (RI/RD onset) and end (RI/RD completion) of each 24-h period. Table 2 shows the basic conditions of the selected samples.

4.1 Geopotential height

From the 200-hPa height field (not shown), the RI TCs do not interact with a high-altitude trough during the RI process, and their north-west is controlled by the South Asian High, with the eastern end of the 1250-dagpm geopotential height line of the South Asian High located 12° east of the TC center at the end of RI. The area of the South Asian High is relatively large. During the RD process of the RD TCs, the South Asian High is obviously enhanced at the end of the RD, and the position is more to the east than for RI TCs. The 1250-dagpm geopotential height line is located 30° east of the TC center and distributed in shape of strips.

Figure 2 shows the 500-hPa geopotential height at the beginning and end of the abrupt intensity change of the RI and RD cases. The western Pacific subtropical high (WPSH) is distributed in a strip shape during the RI process of the RI TCs, and the TC center is located at its south side. Due to the active south-eastern airflow on the south side of the WPSH, the convection that drives the TC is likely to strengthen. With the intensification of a TC within 24 h, the western points and main body of the WPSH tend to withdraw eastwards obviously. For the RD cases, the TC center is located on the west side of the WPSH, and its intensity change is less affected by the WPSH. In addition, the 588-dagpm geopotential height line moves eastwards at the end of the RD, indicating that the WPSH is also weakening as the TC rapidly decays.

4.2 Water vapor fluxes

The main energy of a TC as a heat engine comes from the latent heat released by condensation, and the water vapor fluxes in the low levels can closely affect the TC intensity change. Figure 3 shows the 850-hPa wind vectors and

Table 2 List of basic conditions at the beginning of the 24 h periods of selected samples

Class	No. and name	Time	Position	Pressure /hPa	Wind speed /(m·s^{-1})	ΔV_{24}/(m·s^{-1})
RI	8521 (Dot)	1985/10/14/00	11.6°N, 142.3°E	992	20	15
	8807 (Bill)	1988/08/06/06	25.0°N, 128.0°E	998	15	15
	9025 (Mike)	1990/11/10/00	8.6°N, 135.9°E	960	40	20
	0518 (Damrcy)	2005/09/24/06	19.7°N, 114.8°E	980	30	20
	0621 (Chebi)	2006/11/09/06	15.9°N, 131.3°E	1000	15	30
	1319 (Usagi)	2013/09/17/18	17.2°N, 130.7°E	990	23	15
	1601 (Mujigae)	2016/07/04/06	12.8°N, 141.0°E	992	23	17
RD	7908 (Hope)	1979/08/01/06	20.9°N, 121.7°E	910	60	–15
	8504 (Hal)	1985/06/23/06	21.4°N, 117.1°E	965	40	–15
	9003 (Marian)	1990/05/18/00	18.9°N, 114.3°E	965	40	–20
	9521 (Kent)	1995/11/01/18	14.4°N, 126.8°E	925	60	–20
	0713 (Wipha)	2007/09/18/00	24.4°N, 123.6°E	935	55	–25
	0815 (Jangmi)	2008/09/27/12	21.3°N, 124.4°E	910	65	–20
	1614 (Meranti)	2016/09/13/12	20.4°N, 122.9°E	890	75	–20

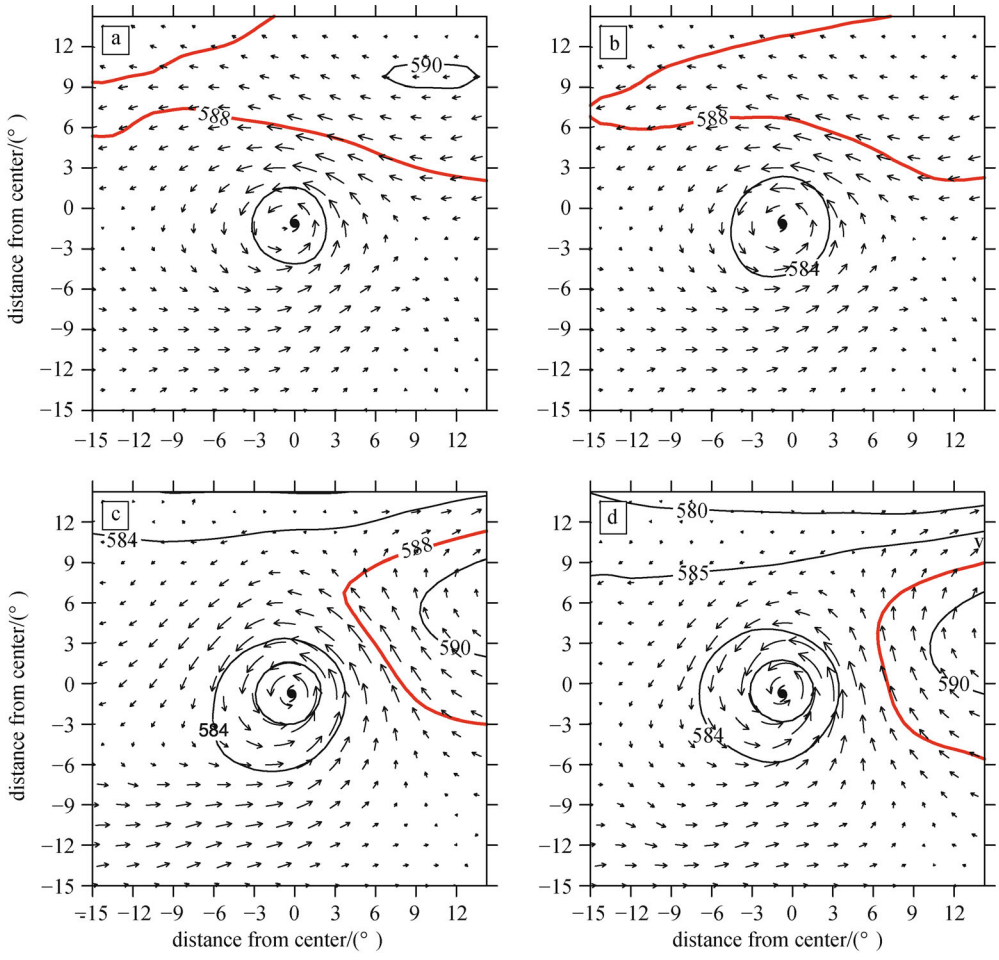

Fig. 2 The 500-hPa geopotential height (solid line) and wind vector (arrows) field of RI and RD TCs (a) at the beginning of RI; (b) at the end of RI; (c) at the beginning of RD; and (d) at the end of RD (units: dagpm). The origin of the coordinates is the TC center; the north and east direction are positive and the south and west are negative.

horizontal water vapor fluxes (contours, giving only a region of no less than 10 g/(s·hPa·cm)). It can be seen that both types of TCs have a south-west jet stream (defined as a strong wind speed zone with a synthetic wind speed of no less than 10 m/s) to deliver warm and moist flow to the TC center during the entire period when abrupt intensity change occurs, and the water vapor supply mainly comes from the ocean to the south. On the south side of the RI TC centers, a strip of water vapor overlays at the south-west jet stream. The water vapor is entangled into the TC center by the south-west airflow, with the maximum value appearing at the north-east of the TC center. Adequate water vapor transport is conducive to maintenance of the warm-core structure of a TC, and providing sufficient energy for TC development.

The water vapor fluxes of the RD TCs are quite different from those of the RI TCs. The speed of the south-west jet stream and the water vapor transport are relatively weak during the RD process, and there is some water vapor flowing out with the westward airflow. These factors are clearly not conducive to TC development.

4.3 Vertical wind shear

Gray and Brody (1967) proposed that, for TCs close to maturity, moderate environmental wind shear is conducive to air pumping of the upper-layer inflow and the bottom-layer outflow, which are favorable for the maintenance and development of TC intensity. Paterson et al. (2005) pointed out that TCs have more possibility to intensify when the vertical wind shear is less than 10 m/s. The presence of significant vertical wind shear will advect heat and moisture away from the TC convection center and then inhibit TC development (DeMaria, 1996).

In the present study, the differences in zonal wind vectors between 200 and 850 hPa are used to compute the vertical wind shear. The distribution of vertical wind shear at the beginning and end of RI/RD cases and their differences are shown in Fig. 4. The results clearly show that the vertical wind shear increases insignificantly for RI TCs during the 24-h periods, with the westerly shear zone located on the north side of the TC center and the easterly shear on the opposite side. The TC center is located at the

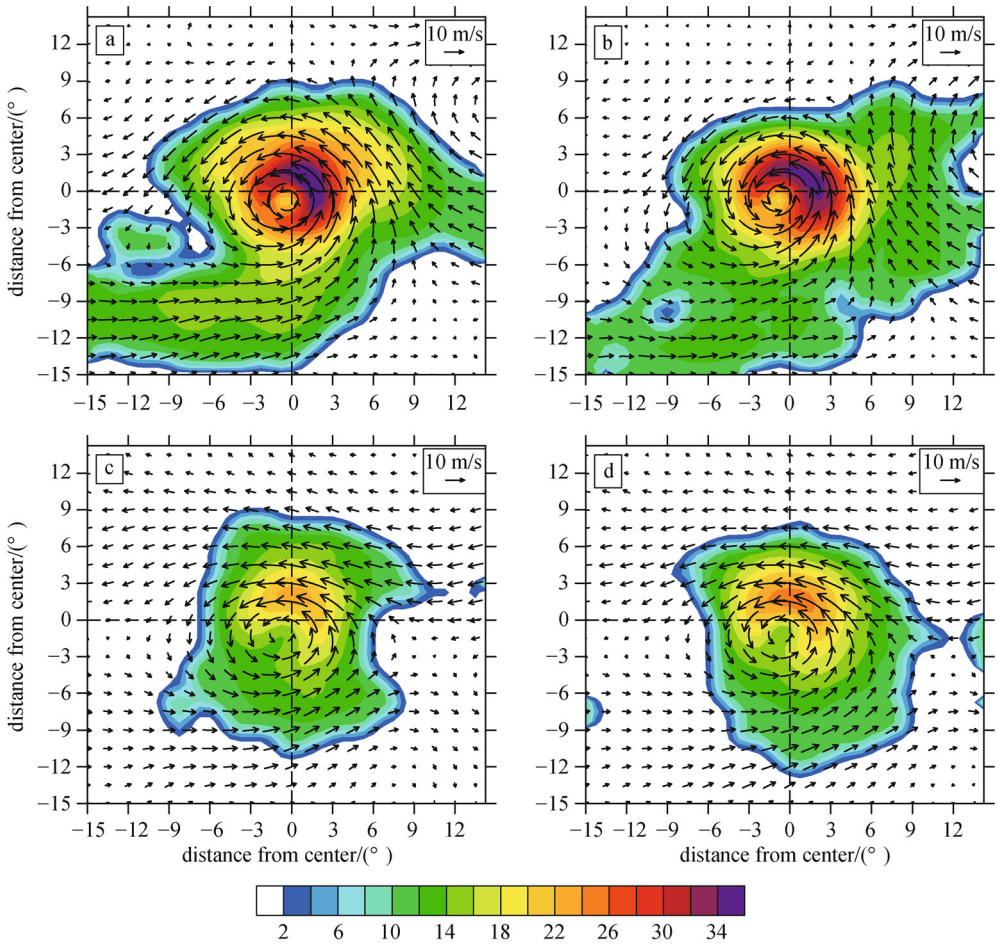

Fig. 3 The 850-hPa wind and water vapor fluxes of the RI and RD TCs (a) at the beginning of RI, (b) at the end of RI, (c) at the beginning of RD, and (d) at the end of RD (units: g/(s·hPa·cm)).

junction of the easterly and westerly wind shear, and a small vertical wind shear is favorable for TC intensification. For the RD TCs, the distribution of vertical wind shear resembles the pattern of RI, but with a lightly larger value. With the development of a TC, the easterly shear increases and the westerly shear changes little. Thus, the meridional gradient of vertical wind shear increases during the RD process, which is not conducive to TC development.

4.4 Relative vorticity

Figure 5 shows the zonal cross sectional structure along the TC center of the selected samples. It is clear that there is a cyclonic vorticity column near the TC center, with the maximum value appearing in the middle-to-low troposphere. Shaded areas indicate upper-tropospheric divergence, while lower-tropospheric convergence.

The relative vorticity and divergence change significantly during the 24-h periods for the RI TCs. At the beginning of RI, there is a large value of cyclonic vorticity ($\sim 2.0\times10^{-5}$/s) from the middle to low level of the troposphere, and an upper-tropospheric divergence zone on the left-hand side of the TC center is also pronounced. Both of these factors are conducive to ascending motion, which is favorable for a TC's development of convection. At the end of the RI, the cyclonic vorticity at the low level weakens and the upper-level divergence zone enlarges slightly. The RI TCs are generally located to the south-west or south of the WPSH. The south-east airflow of the WPSH and the south-west low-level jet stream combine to form convergent conditions in the mid and lower troposphere, which are conducive to TC intensification.

Compared to the RI TCs, the RD TCs have a weaker cyclonic vorticity in the middle-to-low level of troposphere, and a larger upper-tropospheric divergence zone at the beginning of RD. However, with the development of the TC, the lower-level convergence and upper-level divergence are significantly weakened, which is unfavorable for the maintenance of the TC warm-core structure. One possible reason is that the RD samples are generally dominated by easterly airflow at low latitudes in the upper-level troposphere, and the divergence is not robust. Meanwhile, in the middle to lower level, the RD TCs are

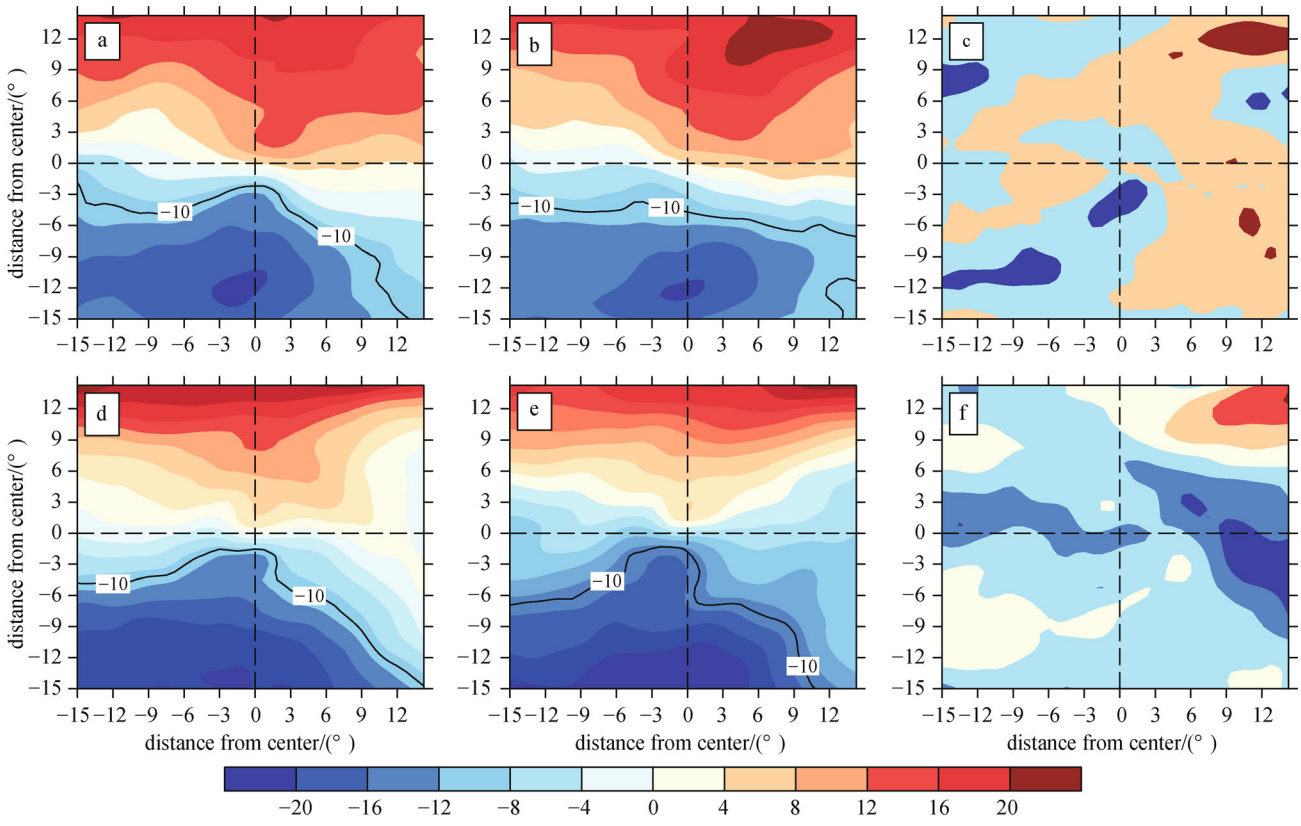

Fig. 4 Vertical wind shear of RI and RD TCs (a) at the beginning of RI; (b) at the end of RI; (c) difference between the beginning and end of RI; (d) at the beginning of RD; (e) at the end of RD; and (f) difference between the beginning and end of RD (units: m = s).

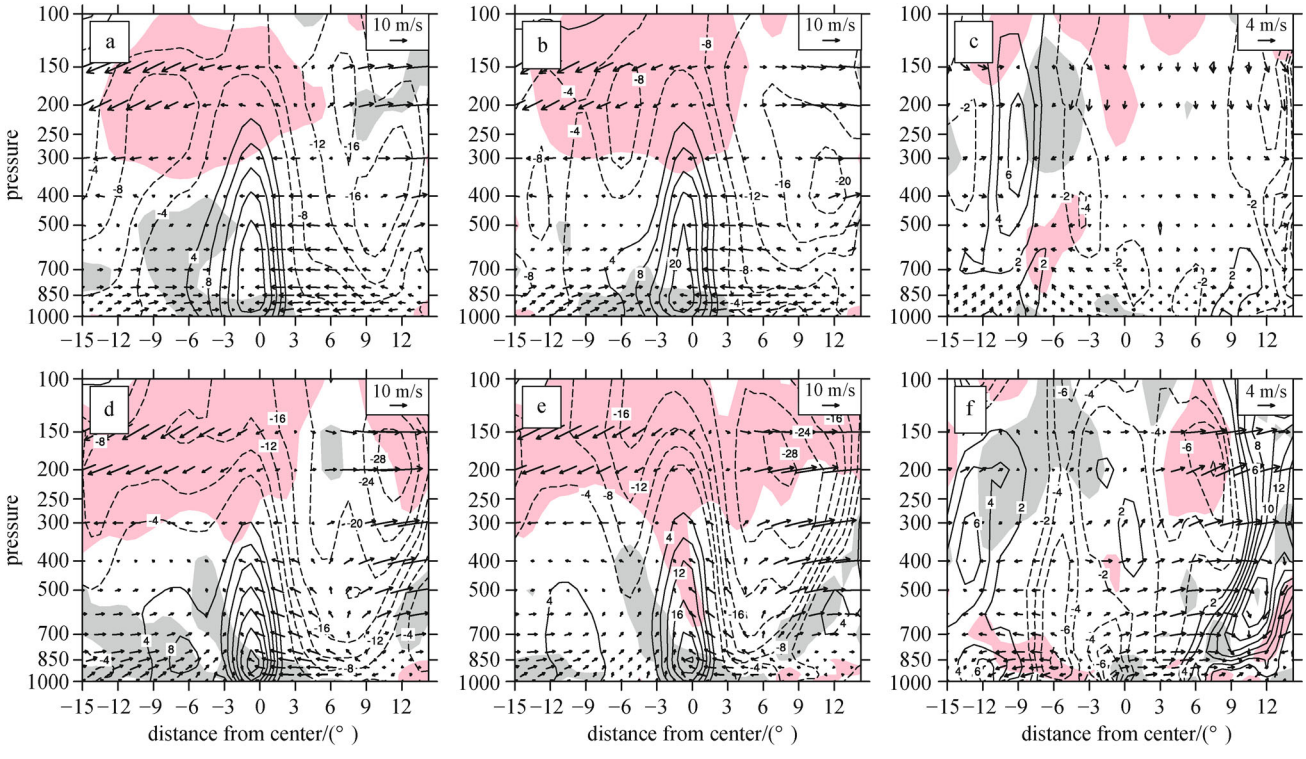

Fig. 5 Relative vorticity (contours; units: $\times 10^{-6}$ /s) and divergence (shaded; red: $\geqslant 1.5 \times 10^{-6}$ /s, gray: $\leqslant -1.5 \times 10^{-6}$ /s) latitudinal-vertical profile of RI and RD TCs (a) at the beginning of RI; (b) at the end of RI; (c) difference between the beginning and end of RI; (d) at the beginning of RD; (e) at the end of RD; and (f) difference between the beginning and end of RD (units: /s).

generally located in the west of the WPSH and the easterly winds are small, combined with slight south-westerly flow, leading to the weak convergence in the mid-to-low level of the troposphere. Such tropospheric conditions are unfavorable for the development of convection, thus contributing to the TCs' RD.

5 Summary and discussion

Data from the CMA and ERA-Interim are employed in this study to examine the large-scale characteristics of landfalling TCs with abrupt intensity change. The results show that of all 657 landfalling TCs during 1979–2017, 71%, 70% and 65% of all landfalling TDs, TSs and TYs, respectively, intensify. Of all the 16595 samples, 4.0% and 0.2% of TYs and TSs, respectively, undergo over-water RI during their lifetime. At the same time, 4.5% and 0.6% of TYs and TSs, respectively, experience over-water RD. In addition, abrupt intensity changes of landfalling TCs are more likely to occur in stronger systems. RI and RD cases occur most in TYs, and most of them intensify with a ΔV_{24} in the range of 15–20 m/s, or decay with a ΔV_{24} in the range of −20 to −15 m/s. East of the Philippine Islands (10°N–15°N, 130°E) is the region with the most frequent occurrence of RI cases, while such cases rarely occur in the South China Sea. More RD cases occur in areas close to the coast compared with open-ocean, and they move to the north-west mostly. In terms of seasonal distribution, most of RI cases (nearly 28%) occur in July. RD cases occur mostly in September (about 29%).

A TC's intensity is generally affected by the presence of favorable environmental conditions. Here, two kinds of cases — namely, RI and RD TCs — are used to examine the environmental conditions associated with them. Comparisons show that the RI cases are generally on the south side of the strong WPSH; the SSTs near the composite TC center at the beginning of RI are marginally conducive to TC development (~29.03°C) but drop about 0.37°C within 24 h (Table 3). Simultaneously, the low-level water vapor fluxes increase, implying that the composite TC gains sufficient moisture during RI. Both the warm SST and sufficient water vapor fluxes appear to precede RI onset. On the contrary, the RD TCs are located on the west side of the WPSH; the SSTs near the TC center are smaller but the decreases during 24-h periods are more dramatic than for the RI cases. Water vapor flux changes are less pronounced, as low-level water vapor transport rarely wraps into the TC circulation from the west and it drops within the entire composite TC. Significant decreases in SSTs might be one plausible cause of the RD. By the time RD begins, the TC has a moderate SST and has begun to lose its source of moisture. This implies that negative environmental factors might be affecting the TC's RD.

In addition, dynamic factors (low-level vorticity and vertical wind shear) have an important effect on the TC intensity change. There are no significant differences in vertical wind shear between the RI and RD cases, implying that this variable is not the key factor that differentiates TCs with abrupt intensity change. However, for RD TCs, the pronounced increasing vertical wind shear during the entire 24-h periods may contribute to the RD onset. Simultaneously, the low-level relative vorticity near the RI TC center at 0 h is moderate for intensifying TCs and increases as the TC develops, implying that the composite TC has enough potential to develop. Conversely, the RD TC center is subjected to a large relative vorticity and negative differences between the end and beginning of RD. This indicates that decreasing low-level relative vorticity may contribute to RD.

In short, the environmental fields of two types of TCs with over-water RI and RD before making landfall have been compared, and some preliminary conclusions drawn. The existence of warm SSTs is a dominant feature for the RI samples that is conducive to the TC development. Sufficient water vapor fluxes involved in the TC circulation also provides enough energy for TCs to intensify. Also, moderate low-level relative vorticity is favorable for TC intensification. On the other hand, a significant decrease in SST and low-level water vapor transport may synergistically contribute to RD. Simultaneously, low-level relative vorticity seems to be unfavorable for TC development, and the combination of these factors amplifies the weakening rate enough to reach the RD threshold. However, the causes of abrupt intensity change in TCs are more complicated. Every TC has its own special internal structure and forcing from different external

Table 3 The mean values of synoptic variables at the initial (t = 0) time and average differences between end and beginning of the RI and RD samples. The differences between these mean values (D = RD − RI) are also shown. The algorithm is applied within 550 km of the TC center. An asterisk indicates statistical significance at the 95% confidence level

Variable	RI		RD		D = RD − RI
	beginning	differences	beginning	differences	
SST/°C	29.03	−0.37	28.19	−0.78*	−0.84*
Water vapor fluxes/(g/(s·hPa·cm)$^{-1}$)	23.38	1.43	15.88	−0.63	−7.50*
vertical wind shear/(m·s^{-1})	0.51	0.39	0.53	0.98	0.02
850 hPa relative vorticity/(10^{-6} ·s^{-1})	25.31	0.38	34.93	−1.95	9.62

environments. The causes of intensity change are not the same, and this paper only shows a commonality. Further research is needed on the impacts of land/terrain on the large-scale characteristics of TC RI/RD, the interaction between TC circulation and TC structural change adjustment of the circulation field.

Acknowledgements This research was supported by the Strategic Priority Research Program of the Chinese Academy of Sciences (Grant No. XDA20060503), the Fund of Southern Marine Science and Engineering Guangdong Laboratory (Zhanjiang) (No. ZJW-2019-08), the National Key R&D Program of China (Grant Nos. 2018YFA0605604 and 2017YFC1501802), the Project of Enhancing School with Innovation of Guangdong Ocean University (No.230419053), the Projects (Platforms) for Construction of Top-ranking Disciplines of Guangdong Ocean University (No.231419022), the Young Innovative Talents Project in Common Colleges and Universities in Guangdong Province (No. 2016KQNCX061). We also thank the CMA, NOAA and ECMWF for the availability of the data used in this work.

References

Bosart L F, Velden C S, Bracken W E, Molinari J, Black P G (2000). Environmental influences on the rapid intensification of Hurricane Opal (1995) over the Gulf of Mexico. Mon Weather Rev, 128(2): 322–352

Chan J C L, Duan Y, Shay L K (2001). Tropical cyclone intensity change from a simple ocean-atmosphere coupled model. J Atmos Sci, 58(2): 154–172

DeMaria M (1996). The effect of vertical wind shear on tropical cyclone intensification change. J Atmos Sci, 53: 2076–2088

Elsberry R L, Lambert T D B, Boothe M A (2007). Accuracy of Atlantic and eastern North Pacific tropical cyclone intensity forecast guidance. Weather Forecast, 22(4): 747–762

Elsberry R L (2014). Advances in research and forecasting of tropical cyclones from 1963–2013. Asia-Pacc J Atmos Sci, 50(1): 3–16

Emanuel K A (1999). Thermodynamic control of hurricane intensity. Nature, 401(6754): 665–669

Emanuel K, DesAutels C, Holloway C, Korty R (2004). Environmental control of tropical cyclone intensity. J Atmos Sci, 61(7): 843–858

Gray W M, Brody L R (1967). Global view of the origin of tropical disturbances and storms. Atmospheric Sci Pape, 114

Huang W, Liang X (2010). Convective asymmetries associated with tropical cyclone landfall; β-plane simulations. Adv Atmos Sci, 27(4): 795–806

Jiang H (2012). The relationship between tropical cyclone intensity change and the strength of inner-core convection. Mon Weather Rev, 140(4): 1164–1176

Kaplan J, DeMaria M (2003). Large-scale characteristics of rapidly intensifying tropical cyclones in the North Atlantic basin. Weather Forecast, 18(6): 1093–1108

Kaplan J, DeMaria M, Knaff J A (2010). A revised tropical cyclone rapid intensification index for the Atlantic and eastern North Pacific basins. Weather Forecast, 25(1): 220–241

Liang J, Wu L, Gu G (2018). Rapid weakening of tropical cyclones in monsoon gyres over the tropical western North Pacific. J Clim, 31(3): 1015–1028

Lin I I, Wu C C, Emanuel K, Lee I H, Wu C R, Pun I F (2005). The interaction of Super Typhoon Maemi (2003) with a warm ocean eddy. Mon Weather Rev, 133(9): 2635–2649

Lowag A, Black M L, Eastin M D (2008). Structural and intensity change of Hurricane Bret (1999). Part I: environmental influences. Mon Weather Rev, 136(11): 4320–4333

Merrill R T (1988). Environmental influences on hurricane intensification. J Atmos Sci, 45(11): 1678–1687

Paterson L A, Hanstrum B N, Davidson N E, Weber H C (2005). Influence of environmental vertical wind shear on the intensity of hurricane-strength tropical cyclones in the Australian region. Mon Weather Rev, 133(12): 3644–3660

Pfeffer R L, Challa M (1981). A numerical study of the role of eddy fluxes of momentum in the development of Atlantic hurricanes. J Atmos Sci, 38(11): 2393–2398

Pun I F, Chang Y T, Lin I I, Tang T Y, Lien R C (2011). Typhoon-ocean interaction in the Western North Pacific, Part 2. Oceanography (Wash DC), 24(4): 32–41

Reynolds R W, Smith T M, Liu C, Chelton D B, Casey K S, Schlax M G (2007). Daily high-resolution-blended analyses for sea surface temperature. J Clim, 20(22): 5473–5496

Shu S, Ming J, Chi P (2012). Large-scale characteristics and probability of rapidly intensifying tropical cyclones in the western North Pacific basin. Weather Forecast, 27(2): 411–423

Simmons A (2006). ERA-Interim: new ECMWF reanalysis products from 1989 onwards. ECMWF Newsletter, 110: 25–36

Willoughby H E, Clos J A, Shoreibah M G (1982). Concentric eye walls, secondary wind maxima, and the evolution of the hurricane vortex. J Atmos Sci, 39(2): 395–411

Wood K M, Ritchie E A (2015). A definition for rapid weakening of North Atlantic and eastern North Pacific tropical cyclones. Geophys Res Lett, 42(22): 10–091

Yuan T, Jiang H (2010). Forecasting rapid intensification of tropical cyclones in the western North Pacific using TRMM/TMI 37 GHz microwave signal. In: 65th Interdepartmental Hurricane Conference (IHC). Miami, USA

Zhang Q, Wu L, Liu Q (2009). Tropical cyclone damages in China 1983–2006. Bull Am Meteorol Soc, 90(4): 489–496